TISSUE ENGINEERING: Part A
Volume 19, Numbers 11 and 12, 2013

DOI: 10.1089/ten.tea.2012.0230

Stiffness-Modulated Water Retention and Neovascularization of Dermal Fibroblast-Encapsulating Collagen Gel

Jae Hyun Jeong, PhD,[1] Youyun Liang, PhD,[1] Michelle Jang, BS,[1] Chaenyung Cha, PhD,[1] Cathy Chu, PhD,[1,3] Haekwang Lee, PhD,[5] Woonggyu Jung, PhD,[6] Jin Woong Kim, PhD,[7] Stephen A. Boppart, MD, PhD,[2,4] and Hyunjoon Kong, PhD[1,3,4]

There is increasing evidence that matrix stiffness modulates various phenotypic activities of cells surrounded by a three-dimensional (3D) matrix. These findings suggest that matrix stiffness can also regulate dermal fibroblasts activities to remodel, repair, and recreate skin dermis, but this has not yet been systematically demonstrated to date. This study examines the effects of matrix rigidity on the morphology, growth rates, and glycosaminoglycan (GAG) production of dermal fibroblasts cultured in collagen-based hydrogels with controlled elastic moduli. The elastic moduli (E) of collagen hydrogels were increased from 0.7 to 1.6 and 2.2 kPa by chemically cross-linking collagen fibrils with poly(ethylene glycol) disuccinimidylester. Increasing E of the hydrogel led to decreases in cellular spreading, nuclear aspect ratio, and growth rate. In contrast, the cellular GAG production level was elevated by increasing E from 0.7 to 1.6 kPa. The larger accumulation of GAG in the stiffer hydrogel led to increased water retention during exposure to air, as confirmed with magnetic resonance imaging. Additionally, in a chicken chorioallantoic membrane, a cell-encapsulating hydrogel with E of 1.6 kPa created dermis-like tissue with larger amount of GAG and density of blood vessels, while a cell–hydrogel construct with E of 0.7 kPa generated scar-like tissue. Overall, the results of this study will be highly useful for designing advanced tissue engineering scaffolds that can enhance the quality of a wide array of regenerated tissues including skin.

Introduction

Many previous studies report that mechanical stiffness of a cell-adherent extracellular matrix (ECM) acts as an insoluble signal to regulate diverse cellular phenotypic activities, including proliferation, differentiation, and gene expression via specific integrin–ligand linkages.[1–5] For example, cells that adhere to stiffer adhesion substrates grow more actively, and cell growth rates are mediated by other matrix properties and multiple soluble factors.[6] In contrast, differentiation of certain stem and precursor cells to a specific lineage is maximized on a substrate with stiffness comparable to specific tissue stiffness.[7] These findings imply that mechanical stiffness of a tissue engineering scaffold designed to induce host cell migration or to transplant cells should act as a bioactive cue to regulate cellular activities critical for tissue regeneration.

Extensive efforts have been made to understand the role of matrix stiffness in regulating phenotypic activities of a variety of cells encapsulated in a three-dimensional (3D) matrix.[8–10] Toward this end, various hydrogels with interfibrillar networks, such as fibrin and collagen gel, are being designed with controllable stiffness to examine cellular activities.[10–13] The stiffness of collagen hydrogels is typically controlled using short cross-linkers with bivalent or multivalent aldehyde groups; however, these methods are toxic to cells.[10–11] Therefore, it is common to first induce interconnected micropores into the hydrogel via lyophilization or porogen leaching, and subsequently incorporate cells into the pores. However, this approach may not precisely reflect the 3D microenvironment of cells in the original tissue. Therefore, enzymatic cross-linkers are used to control stiffness of the cell-encapsulated fibrin or collagen gels, while circumventing concerns on toxicity. However, these cross-linkers do not control gel stiffness over a physiologically relevant range.[12–13]

We have recently demonstrated that poly(ethylene glycol) dissucinimidyl ester (PEGDE) can be used as a biocompatible cross-linker for cell-encapsulating collagen gels.[14] This approach resulted in changes in stiffness without significantly

[1]Department of Chemical and Biomolecular Engineering; [2]Departments of Bioengineering, Electrical and Computer Engineering, and Medicine; [3]Institute for Genomic Biology; [4]Beckman Institute for Advanced Science and Technology, University of Illinois at Urbana–Champaign, Urbana, Illinois.
[5]Amore Pacific R&D Center, Yongin, Republic of Korea.
[6]School of Nano-Bioscience and Chemical Engineering, Ulsan National Institute of Science and Technology (UNIST), Ulsan, Republic of Korea.
[7]Department of Applied Chemistry, Hanyang University, Ansan, Republic of Korea.

changing molecular diffusivity through the gel matrix, which may also influence cellular activities in a 3D matrix coupled with gel stiffness. These hydrogels were used to examine effects of gel stiffness on malignant activities of cancer cells. However, it was not examined whether the stiffness of this hydrogel influences phenotypic activities of normal cells required for tissue remodeling and regeneration.

Using these collagen–PEGDE hydrogels with varied elastic moduli, this study demonstrates that the elastic modulus of the hydrogel can regulate cellular activities required to recreate new skin tissue. In this study, dermal fibroblasts were encapsulated into collagen hydrogels reinforced with varying concentrations of PEGDE cross-linkers. We first examined the effects of the elastic moduli of the hydrogel on cell morphology, growth rate, and sulfated glycosaminoglycan (GAG) expression, all of which are significantly involved in skin tissue regeneration and remodeling.[15] In natural tissues, GAG molecules, polysaccharide components, are known to play critical roles in both structural integrity and water retention of an ECM, because of their repeating disaccharide units and hydrophilic groups.[16–18] Therefore, the capability of the cell–hydrogel construct to retain water was evaluated using magnetic resonance imaging (MRI), following *in vitro* cell culture over 14 days. Finally, the cell–hydrogel construct was implanted on a chicken chorioallantoic membrane (CAM) over 7 days, and the remodeled construct was imaged using 3D optical coherence tomography (OCT) and histological staining. Taken together, this study serves not only to disclose the crucial role of 3D matrix stiffness in cellular activities, but also to provide an advanced tissue engineering platform to improve the quality of a wide array of regenerated tissue.

Materials and Methods

Preparation of collagen and collagen–PEG hydrogels

Pure collagen gels were prepared by mixing prechilled bovine collagen type I solution (3.0 mg/mL, Advanced BioMatrix), Medium 106 (M106, Life Technologies), and reconstituting solution in a ratio of 8:4:1. The reconstituting solution was a mixture of 0.26 M of sodium bicarbonate, 0.2 M 4-(2-hydroxyethyl)-1-piperazineethanesulfonic acid, and 0.04 M of sodium hydroxide. The mixture was subsequently incubated in a 96-well plate at 37°C for 4 h to form 3D collagen hydrogels with 4.3 mm diameter and 1 mm thickness. To prepare collagen–PEG hydrogels, PEGDE (M_w ~446 g/mol; Sigma-Aldrich) was dissolved in dimethyl sulfoxide at 50 mg/mL. The solution was then added to collagen/M106/reconstituting solution mixture. The final PEGDE-to-collagen mass ratio ($M_{PEG\text{-}COL}$) was varied from 0.33 to 1.00.The mixture was incubated at 37°C for 4 h to induce gel formation. All procedures were performed under sterile conditions. The resulting gel was incubated in M106 until characterization, and the medium was replaced with a fresh medium every 3 days.

Characterizations of stiffness of and molecular diffusivity within hydrogels

The stiffness of the collagen-based hydrogel was evaluated with measurement of the elastic modulus (E) of a hydrogel using a mechanical testing system (Insight). The hydrogels were compressed at a rate of 1.0 mm·min^{-1}, and the elastic modulus was calculated from the linear slope of a stress (σ) versus strain (λ) curve at the first 10% strain. Four samples were measured per condition. Biomolecular diffusivity within gels was determined by fluorescence recovery after photobleaching (FRAP) assay. The FRAP experiments were performed on a multiphoton confocal microscope, equipped with FRAP module (Zeiss LSM 710).[19] Fluoresceinisothiocynate (FITC)-dextran (molecular weight ~40 or 500 kDa) was incorporated into the gels as a fluorescent probe. Three randomly selected circular spots each with diameters of 85 μm were photo-bleached with a short-pulsed 488-nm laser. The bleaching iterations were adjusted so that the resulting fluorescence from the spot became ~60% of the original fluorescence. The recovery of fluorescence intensity over time was measured and the curve was fitted with the following equation:

$$f(t) = A + Bexp\left(-\frac{2T}{t}\right) \quad (1)$$

where $f(t) = \frac{F(t)}{F_0}$, F_0 is initial fluorescence before bleaching, $F(t)$ is fluorescence intensity at a given time, t, T is the recovery time constant, A is the initial fluorescence yield, and B is a modified Bessel function. The diffusion coefficients (D) of FITC–dextran within the respective gels were then calculated with the following equation:

$$D = \frac{r^2}{4T} \quad (2)$$

where D is the diffusion coefficient of FITC–dextran (cm^2/sec) and r is the radius of cylindrical bleached spots.

Human dermal fibroblasts culture and assays in hydrogels

Primary human dermal fibroblasts (HDFs, American Type Culture Collection [ATCC]) with passage number lower than three were used in this study. The HDFs were cultured in M106 medium supplemented with 2% (v/v) low serum growth supplement (Life Technologies) and 1% (v/v) penicillin–streptomycin (Gibco). The cells were maintained at 37°C in a 5% CO_2 and 95% relative humidity environment. The medium was exchanged with a fresh medium every 3 days. For cell encapsulation, cells were mixed with collagen and reconstituting solutions; 0.33, 0.66, and 1.0 mg PEGDE/mg collagen were added to generate collagen–PEG hydrogels with different elastic moduli. The final cell density in the gel was 2×10^6 cells/mL. After incubation for 4 h to allow hydrogel formation, an additional culture medium was added to the gel. The medium was exchanged every 3 days. On days 0, 1, 4, 7, 10, and 14, the number of metabolically active viable cells in the hydrogel was evaluated using a 3-(4,5-dimethylthiazol-2-yl)-2,5-diphenyltetrazolium bromide (MTT) reagent (ATCC) assay kit. The cell–hydrogel construct was incubated in the medium containing MTT reagent for 4 h, and the absorbance of the sample altered with the positively stained viable cells was subsequently measured at 570 nm using a microplate absorbance reader (Synergy HT, Biotek). The absorbance measured at days 1, 4, 7, 10, and 14 was normalized to that measured at day 0 to quantify the relative cellular metabolic activity.

After 3 days of culture, cell–hydrogel constructs were fixed using a 4% formaldehyde solution (Fisher Scientific) overnight at room temperature. Following blocking, the cells were incubated with 4,6-diamindino-2-phenylindole (DAPI, Sigma Aldrich) and their respective antibodies. For imaging of actin filaments, rhodaminephalloidin (Molecular Probes) was used. For imaging of β1-integrin, mouse monoclonal β1-integrin antibody and goat polyclonal antibody conjugated with Cy5 (Abcam) were used as the primary and secondary antibodies, respectively. After staining with the respective antibodies, the samples were washed with phosphate buffered saline (PBS) and imaged with the multi-photon confocal microscope (Zeiss LSM 710) using the 2-photon mode for phalloidin and the single-photon mode for β1-integrin imaging.

The cellular production of sulfated GAG molecules was evaluated by exposing the cell–hydrogel constructs to alcian blue 14 days after cell culture in the hydrogels.[20] The cell–hydrogel constructs were washed with PBS three times and immersed in 4% paraformaldehyde solution for 10 min. Then, the constructs were exposed to alcian blue (0.05% w/v, Fluka) dissolved in 50 mM sodium acetate buffer containing 50 mM $MgCl_2$ (pH 5.8) overnight at room temperature. The complexes formed from interaction between the cell-secreted GAG molecules and alcian blue dyes were isolated by centrifugation at 6000 rpm for 15 min. The separated complexes were dissociated by mixing them with sodium dodecyl sulfate (40% w/v) in sodium acetate buffer for 5 min. Finally, optical density of the extracted dye was measured at 650 nm in a 96-well plate reader. Using a standard curve created with chondroitin sulfate C (Sigma), the GAG concentration in the hydrogel was back calculated from the optical density.

Analysis of microstructure of hydrogels using scanning electron microscopy

Cross sections of collagen hydrogels and HDF-encapsulating hydrogels were examined using scanning electron microscopy (SEM, JEOL 7000F SEM). After 7 and 14 days of cell culture, the HDF-encapsulating collagen gels were fixed with a 4% formaldehyde solution (Fisher Scientific) at room temperature. The fixed samples were washed with PBS several times and finally washed with distilled water. Then, all samples were flash-frozen using liquid nitrogen, fractured, and lyophilized for imaging. Cross sections of samples were coated with gold in a sputter coater, and the surface morphology was examined at electron intensity of 10 kV with SEM.

Analysis of water evaporation from gels using MRI

Water evaporation from cell–hydrogel constructs cultured in vitro was examined by measuring the local amount of water proton in the hydrogel with the MRI. Following cell culture in the hydrogel over 14 days, MRI scanning of the hydrogel was carried out using 600 MHz Varian Unity/Inova nuclear magnetic resonance (NMR) spectrometer (14.1 T Magnet) at room temperature. The gel was inserted into an radio frequency coil. Spin echo multi-slice pulse sequence was used to acquire resonance data, which was then converted into a water density map using the VNMR 6.1C software. The amount of water protons imaged with MRI was quantified using ImageJ software.

In vivo *implantation of the cell–hydrogel constructs and analysis of imaged explants*

The application of these cell–collagen hydrogel constructs for tissue regeneration was examined by implanting the cell–hydrogel construct onto chicken CAM according to a previously developed method.[21] Briefly, fertilized chicken eggs (Hy-Line W-36) were obtained from the University of Illinois Poultry Farm. Following the initial incubation, a small window (1.0×1.0 cm) was created by removing a portion of the shell on top of each egg. Following the culture of cell-seeded hydrogels over 1 week *in vitro*, the cell–hydrogel constructs were subsequently implanted on the CAM of individual embryos. The diameter and thickness of the hydrogel were kept constant at 10 and 1 mm, respectively. After incubation for 7 days, the membrane was fixed with 10% neutral buffered formalin to image the vascular structure. The fixed membrane was also embedded in paraffin and tissue sections were stained with hematoxylin and eosin (H&E) and Alcian blue. The inflammatory response was also assessed by quantifying the area occupied by immune cells and fibrotic tissue.

Separately, 3D images of the gel explants were acquired using a high-resolution spectral domain OCT system.[22] The OCT system in this study utilized a Ti:Sapphire laser as the optical source, having a spectral bandwidth of 100 nm full-width-half-maximum and a center wavelength of 800 nm, providing ~2 μm axial resolution in tissue. The transverse resolution of the system was 10 μm, based on the focusing optics in the sample arm. Light from this source was guided into one port of the 2×2 fiber coupler, and split into a reference path and an imaging path to the sample. Reflected signals from each path were recombined by the 2×2 fiber coupler and the resulting spectral interference was captured by a high-speed spectrometer. The size of the acquired 3D volume was 7 mm×7 mm×1.5 mm, with 2,048 axial sampled points in depth along each depth-scan, and with each cross-sectional image composed of 1,500 depth-scans.

Statistical analysis

Statistical significance was determined using one-way ANOVA followed by Tukey's Multiple Comparison Test ($p < 0.05$).

Results and Discussion

Characterization of the collagen–PEG hydrogel

Hydrogels were prepared by inducing physical association between collagen molecules to form interconnected fibrous networks and subsequently cross-linking collagen fibrils with PEGDE, as reported previously (Fig. 1A).[14] According to images acquired with an SEM, incorporation of PEGDE into the collagen gel did not interfere with the collagen fiber formation in the hydrogel. Increasing the mass ratio between PEGDE and collagen ($M_{PEG\text{-}COL}$) from 0 to 1.0 led to an increase of the elastic modulus of the bulk hydrogel (E), characterized by the compressing the hydrogels, from 0.7 to 2.2 kPa, each of which is similar to elastic moduli of fat and dermis, respectively (Fig. 1B).[23,24]

In contrast, according to the FRAP assay, increasing $M_{PEG\text{-}COL}$ from 0 to 0.33 insignificantly decreased the average diffusivity of dextran with molecular weight of 40 kDa within the gel (D_{gel}) from 2.6×10^{-7} to 1.7×10^{-7} cm^2/s, but the

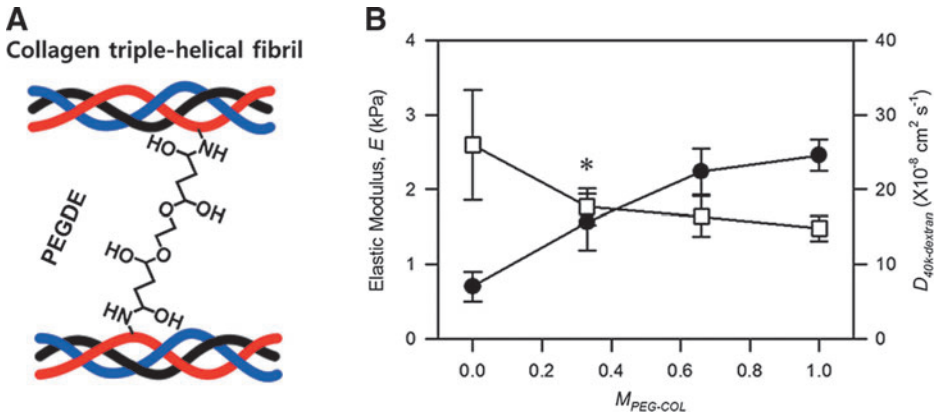

FIG. 1. Preparation and characterization of collagen-poly(ethylene glycol) dissucinimidyl ester (PEGDE) gels with varied mechanical stiffness. **(A)** Schematics to control collagen gel stiffness with PEGDE. Stiffness of the collagen gel is increased by introducing covalent cross-links between collagen fibrils and PEGDE. **(B)** Effects of the mass ratio between PEGDE and collagen ($M_{PEG\text{-}COL}$) on the elastic modulus of the gel, and $D_{40k\text{-}dextran}$ characterized with fluorescence recovery after photobleaching assay. Data points and error bars represent the mean values and standard deviation from four independent experiments. The difference between $D_{40k\text{-}dextran}$ at $M_{PEG\text{-}COL}$ of 0 and $D_{40k\text{-}dextran}$ at $M_{PEG\text{-}COL}$ of 0.33 is not statistically significant (*$p > 0.05$). Color images available online at www.liebertpub.com/tea

difference between two values was not statistically significant (Fig. 1B & Supplementary Fig. S1; Supplementary Data are available online at www.liebertpub.com/tea). A further increase of $M_{PEG\text{-}COL}$ from 0.33 to 1.0 resulted in minimal changes of D_{gel} despite increases in E. In contrast, increasing $M_{PEG\text{-}COL}$ from 0 to 0.33 significantly decreased the average diffusivity of dextran with molecular weight of 500 kDa (Supplementary Fig. S1). Further increase of $M_{PEG\text{-}COL}$ minimally altered the diffusivity of dextran with the higher molecular weight, similar to the dextran with the lower molecular weight. Overall, increasing $M_{PEG\text{-}COL}$ from 0 to 0.33 and 0.67 significantly increased the gel stiffness, while resulting in insignificant changes in gel permeability, specifically for biomolecules with molecular weight lower than 40 kDa.

Effects of gel stiffness on cellular morphology

Based on the hydrogel characterizations reported above, HDFs were encapsulated into hydrogels prepared at $M_{PEG\text{-}COL}$ of 0, 0.33, and 0.67. These formulations were selected because they increased E from 0.7, to 1.6 and 2.2 kPa, while limiting decreases in gel permeability. Cells were mixed with pregel solutions consisting of collagen and varied concentrations of PEGDE, in order to encapsulate them in the gel via *in situ* cross-linking reaction. After 3 and 14 days of cell culture, cells encapsulated in hydrogels with varied E displayed different degrees of actin polymerization, cell nuclear aspect ratio, and β1 integrin expression (Fig 2 & Supplementary Fig. S2). Specifically for cells cultured for 3 days, the extent of cell spreading, characterized by measuring cell surface area, decreased linearly with increasing E (Fig. 2A, C). The nuclear aspect ratio of the cell, which represents cellular contractility, also decreased linearly with increasing E (Fig. 2A, D). In contrast, cells encapsulated in a collagen–PEGDE hydrogel with E of 1.6 kPa exhibited the highest β1 integrin expression level, as compared with cells cultured in the hydrogels with E of 0.7 and 2.2 kPa (Fig. 2B-2 & 2E). The difference of the β1 integrin expression level between the conditions became more significant over time (Fig. 2B-1 & 2E).

These results are quite different from previous findings largely obtained with cells cultured on a 2D substrate. It has been extensively reported that cells adhered onto a stiffer substrate stretch more extensively and also display a nucleus with a higher aspect ratio.[25,26] These increases in cellular surface area and nuclear aspect ratio on the stiffer matrix were attributed to increases in the cellular integrin expression level, which represents an increase in the number of integrin–ligand bonds. In contrast, cells cultured in a 3D hydrogel exhibited a maximal integrin expression at E of 1.6 kPa. This result indicates that the largest integrin–ligand bonds are formed in the hydrogel with intermediate stiffness. However, within a 3D hydrogel, it is likely that cellular activity for membrane and nuclear stretching via integrin anchorage to a matrix is counterbalanced by matrix rigidity. Therefore, the extent of cellular membrane and nucleus stretching may not be always related to the number of integrin–ligand bonds for cells in a 3D hydrogel, unlike cells adhered to 2D substrates.

In addition, the maximal integrin expression and integrin–ligand bonds at an intermediate stiffness of the gel was also reported in previous studies conducted with mesenchymal stem cells encapsulated in an alginate hydrogel, although the intermediate elastic modulus value was different from the one in this study.[27] We attribute the difference of the elastic modulus values between this previous study and ours to be related to the differences in the microstructure of the hydrogel and the cell types. Note that the hydrogel used in this study is an interconnected fibrous collagen hydrogel, while previous studies largely used a hydrogel without interconnected fibrous structures. Additionally, several previous studies reported that the cellular response to matrix stiffness is mediated by cell types.[28–31]

Effects of gel stiffness on the cellular phenotypic activities

The cell proliferation in a 3D hydrogel was evaluated by quantifying the increase in the number of metabolically

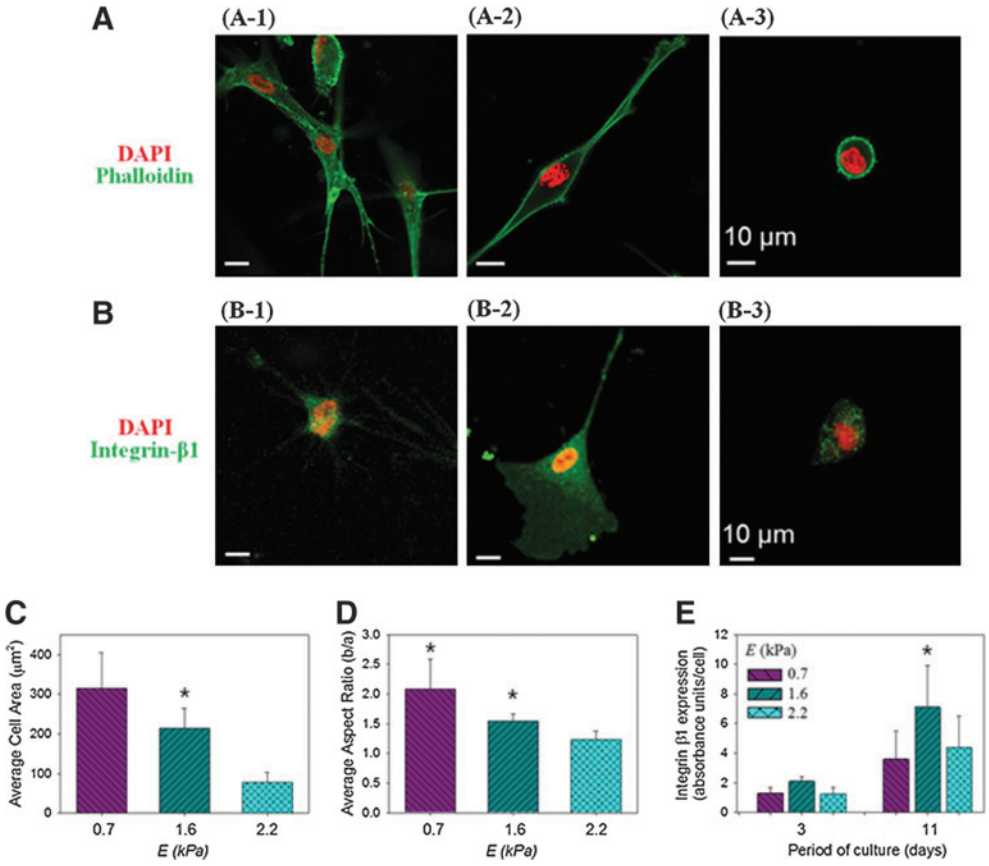

FIG. 2. Effects of gel stiffness on the cellular morphology. **(A)** Fluorescence immunostaining images of human dermal fibroblasts (HDFs) in the hydrogels with varied elastic moduli (E) of 0.7 (A-1), 1.6 (A-2), and 2.2 kPa (A-3). Cell nucleus and intracellular actin were stained with DAPI (blue color) and phalloidin (green), respectively. **(B)** Fluorescence immunostaining images of cellular β1 integrin expression (green) and cell nucleus (blue) in the hydrogels with varied E of 0.7 (A-1), 1.6 (A-2), and 2.2 kPa (A-3).**(C)** Effects of E on the extent of cellular stretching, quantified with the cell area using ImageJ software. The differences between the three conditions were statistically significant (*$p < 0.05$). **(D)** Effects of E on the cellular nucleus aspect ratio, calculated as the ratio of cellular minor axis (width) to major axis (height). The differences between cells encapsulated in the hydrogel with E of 0.7 and 1.6 kPa and those in the hydrogel with E of 2.2 kPa were statistically significant (*$p < 0.05$). All characterizations presented in **(A–D)** were made 3 days after cell encapsulation in the hydrogels. **(E)** Effects of E on the intracellular β1 integrin expression. Integrin expression was examined on days 3 and 11 after cell encapsulation into the hydrogels. On day 11, the differences between cells encapsulated in the hydrogel with E of 1.6 kPa and those in the hydrogel with E of 0.7 and 2.2 kPa were statistically significant (*$p < 0.05$). In all analysis, 150 cells were analyzed for each condition. Color images available online at www.liebertpub.com/tea

active cells, which were identified by positive staining with the reduced MTT salt (Fig. 3A). According to the first assay of the number of viable metabolically active cells conducted 24 h after cell encapsulation, 90% of cells remained viable, independent of E (Fig. 3B). In contrast, during cell culture over 14 days, cells encapsulated within the pure collagen gel with E of 0.7 kPa exhibited a significant increase in the relative cell viability over time (Fig. 3B). Increasing E to 2.2 kPa resulted in a smaller decrease in the relative cellular metabolic activity over time. Therefore, the cell growth rate, quantified with the dependency of the relative cellular metabolic activity on cell culture period, was inversely dependent on E (Fig. 3C). Additionally, the pure collagen gel underwent the larger shrinkage during cell culture than the stiffer collagen–PEG hydrogel, likely because of the active cellular stretching and proliferation (Supplementary Fig. S3).

The E of the hydrogel also tuned the cellular production of sulfated GAG molecules, which was characterized by measuring a concentration of complexes of the cell-secreted GAG molecules and Alcian blue dyes (Fig. 4A). The cell-free hydrogel resulted in no GAG accumulation, as evidenced by no positive signal from the Alcian blue stain. The hydrogels with encapsulated cells, however, exhibited the positive signal of the Alcian blue (Fig. 4A). Increasing E of the cell-encapsulated hydrogel from 0.7 to 1.6 led to a 1.3-fold increase of the total GAG production level (Fig. 4B). Further normalization of the total GAG production level to the number of viable cells, identified with reduced MTT salts, disclosed that increasing E of the hydrogel from 0.7 to 1.6 kPa resulted in an almost two-fold increase of the cellular GAG production level (Fig. 4C). Coupled with FRAP measurement conducted using dextran with molecular weight of 500 kDa, the larger accumulation of GAG in the collagen–PEGDE with E of 1.6 kPa should be attributed to both the larger cellular secretion and the smaller diffusion of GAG.

In parallel, cross sections of the cell–hydrogel constructs were examined by imaging them with SEM. After *in situ* cell encapsulation, the gels displayed interconnected collagen

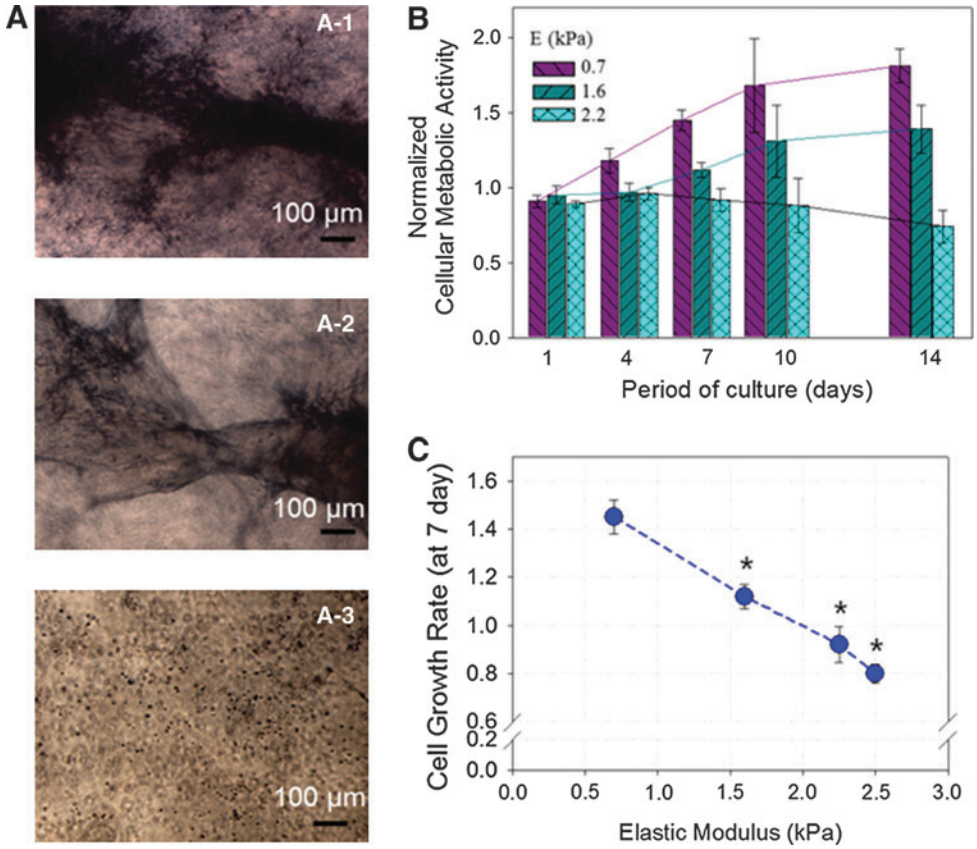

FIG. 3. Effects of gel stiffness on HDF's growth rate. **(A)** Phase-contrast images of HDFs positively stained by 3-(4,5-dimethylthiazol-2-yl)-2,5-diphenyl tetrazolium bromide reagents. Images were captured after 14 days of cell culture. HDFs were encapsulated in collagen–PEGDE gels with varying $M_{PEG\text{-}COL}$ of 0 (A-1), 0.33 (A-2), and 0.67 (A-3). **(B)** Changes in the number of HDFs remained metabolically active in the hydrogels over 14 days. The cellular metabolic activity measured at each time point was normalized to the metabolic activity characterized right after cell encapsulation. All values are mean ± standard deviation of three different samples per condition. **(C)** The cell growth rate, characterized with a slope of the relative cell viability versus cell culture period curve, was inversely related to the elastic modulus (E) of the hydrogel. Statistical significance of the cellular growth rate in the hydrogel with E of 0.7 kPa, relative to cellular growth rates in the hydrogel with E of 1.6 and 2.2 kPa (*$p < 0.05$). Color images available online at www.liebertpub.com/tea

fibers in which the HDFs were entrapped (Supplementary Fig. S4). Following another 7 days of cell culture, the cross section of the cell-encapsulated collagen–PEGDE gel with E of 1.6 kPa showed a new connective matrix formed around the encapsulated HDFs (Fig. 5B-2). In contrast, the pure collagen hydrogel with E of 0.7 kPa did not exhibit any significant change in the microstructure (Fig. 5A-2). Given that GAG concentration was larger in the stiffer collagen–PEGDE gel, it is likely that the matrix formed around the cells is constituted with cell-secreted GAG molecules.

This result therefore demonstrates that dermal fibroblast growth rate and GAG production level are inversely related to each other, suggesting that stiffness of the cell-encapsulated hydrogel is able to tune desired cellular activities in a 3D matrix. Coupled with fibroblast morphology and integrin expression characterized in the previous section, this result also implies that the cellular integrin expression is more closely related to the cellular GAG production, while the extent of cell stretching and nuclear aspect ratio are more closely related to the cellular growth rate. We suggest that the larger number of cellular integrin–ligand bonds formed on the gel with intermediate stiffness stimulated fibroblasts to produce GAG molecules but did not stimulate cellular signaling related to growth. In contrast, the cellular proliferation in a 3D matrix becomes more active as the cells stretch and become more contractile. However, ranges of storage moduli required to activate cellular growth or biomacromolecular production may not be universal to all cell types, because cellular sensitivity to the mechanical environment is known to vary between cell types.

Analysis of water evaporation from the HDF–hydrogel constructs

The cell–hydrogel constructs cultured *in vitro* for 2 weeks were exposed to air to examine whether the GAG molecules secreted by cells and subsequently accumulated within the matrix enhances the capability of the matrix to retain water. Two different hydrogels with E of 0.7 and 1.6 kPa were used in this study, because these two gels resulted in the greatest difference in the cellular GAG production level. The ability of the construct to retain water was examined by monitoring the loss of water bound with a matrix using an MR imaging scanner (Fig. 6). According to the water density map developed with MRI scanning, the cell-free collagen–PEGDE hydrogel with E of 1.6 kPa displayed the faster loss of bound

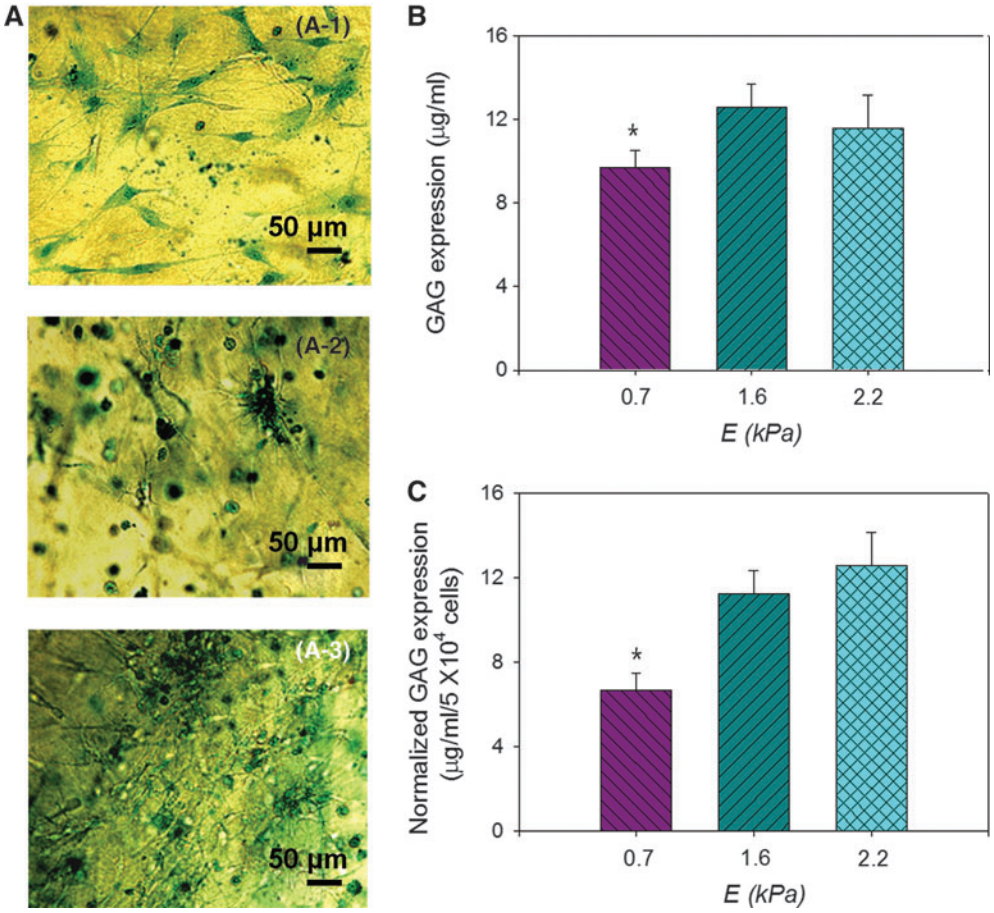

FIG. 4. Effects of gel stiffness on HDF's expression of glycosaminoglycan (GAG). **(A)** Optical microscopic images of GAGs secreted by dermal fibroblasts cultured in hydrogels with varied elastic moduli (E) of 0.7 (A-1), 1.6 (A-2), and 2.2 kPa (A-3). GAG molecules were positively stained by Alcian blue. **(B)** The GAG expression level mediated by E. **(C)** The dependency of normalized GAG expression level on E. In **(C),** the GAG expression level presented in **(B)** was normalized to the number of viable cells. All characterizations displayed in **(A–C)** were conducted 14 days after cell encapsulation. In **(B)** and **(C),** the differences between cells encapsulated in the hydrogel with E of 0.7 kPa and those in the hydrogel with E of 1.6 and 2.2 kPa were statistically significant ($^*p < 0.05$). All values in **(B)** and **(C)** are mean ± standard deviation of four different samples per condition. Color images available online at www.liebertpub.com/tea

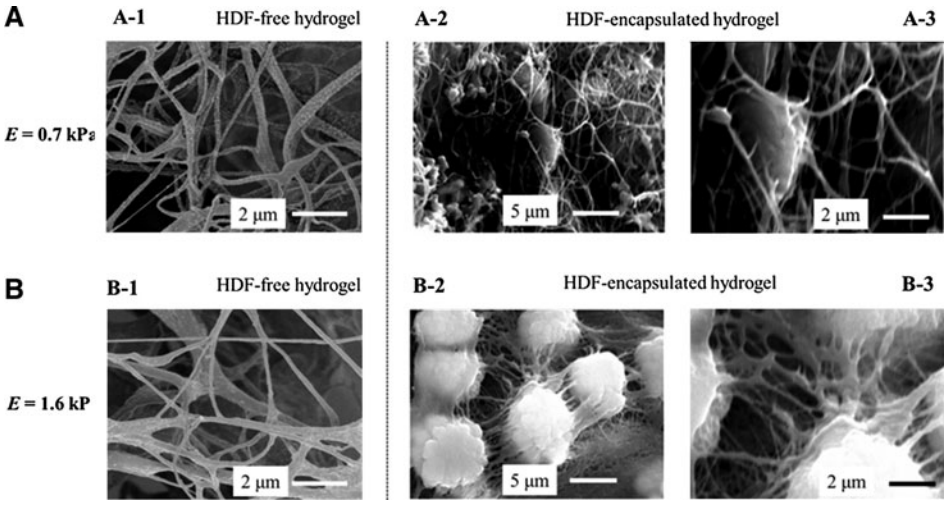

FIG. 5. Scanning electron microscopic (SEM) images of cell-free hydrogels (A-1 and B-1) and HDF-encapsulated hydrogels with varied E of 0.7 **(A)** and 1.6 kPa **(B)**. The microstructure of cell–hydrogel constructs shown in (A-2) and (B-2) were further magnified in (A-3) and (B-3). These images were captured after 14 days of cell culture in the hydrogel. In (B-3), individual circular features represent cells covered with a matrix.

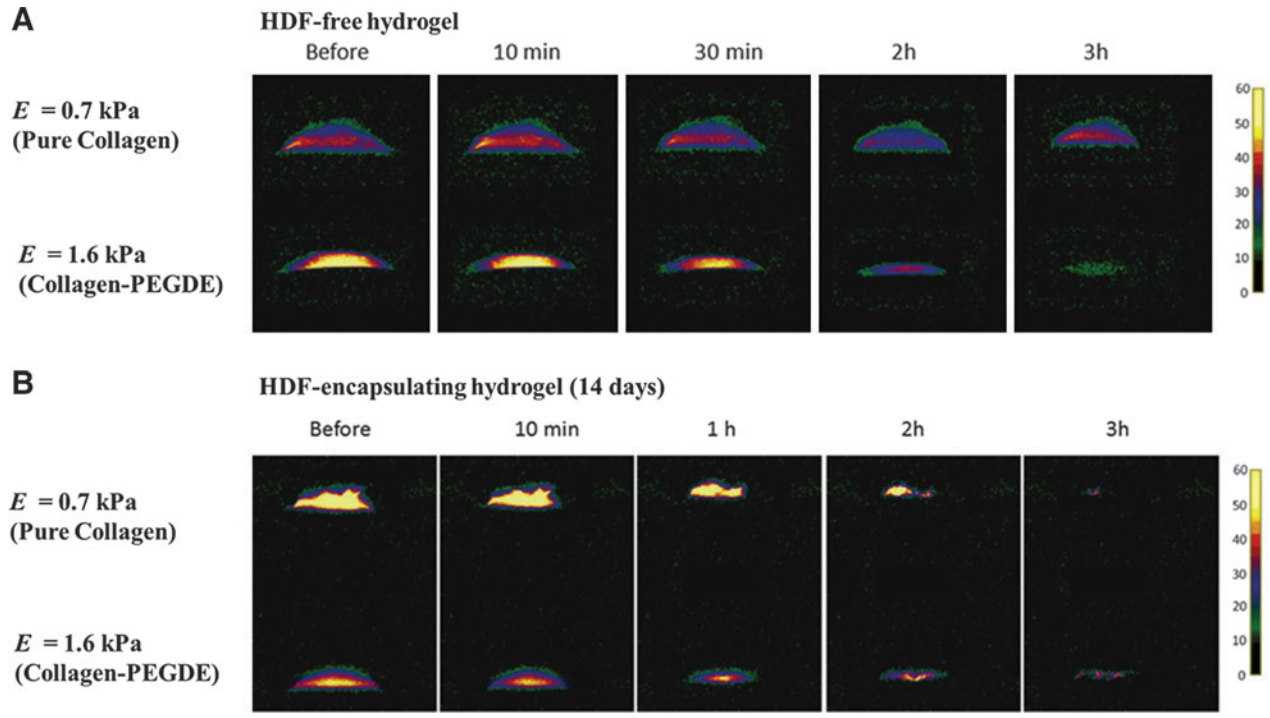

FIG. 6. Magnetic resonance imaging (MRI) analysis of water retention from the HDF-free hydrogels **(A)** and HDF-encapsulating hydrogels **(B).** Pseudo-color of MR images represents the relative peak intensity of water proton. The HDF-encapsulating hydrogels were characterized 14 days after cell culture in the hydrogels. These MRI images were taken at 10 min, 1 h, 2 h, and 3 h after starting to expose the gels to air. A high intensity of yellow color denotes strongly "bound" water molecules, whereas a low intensity of yellow color corresponds to "free" water molecules. Color images available online at www.liebertpub.com/tea

water than the cell-free pure collagen gel with *E* of 0.7 kPa, as noted by the faster disappearance of yellow and red colors (Fig. 6A). In contrast, the cell-encapsulated collagen–PEGDE hydrogel exhibited the slower disappearance of bound water than the cell-encapsulated collagen gel (Fig. 6B). Coupled with the FRAP assay, GAG assay, and SEM images (Figs. 4 and 5), this MR imaging clearly indicates that cell-encapsulated collagen–PEGDE hydrogels more populated with GAG molecules prevented water evaporation, as compared to the softer pure collagen gel.

In vivo *implantation of the HDF–hydrogel constructs*

Following HDF culture in hydrogels with *E* of 0.7 or 1.6 kPa over 1 week *in vitro*, the cell–hydrogel constructs were implanted on the CAM of a chick embryo for over 7 days to examine *in vivo* effects of the matrix rigidity on cellular activities to regenerate vascularized dermis-like tissue. We have limited the entire cell culture and transplantation period to 14 days, because HDFs encapsulated in the gel produce their own matrices over time and ultimately minimize effects of gel rigidity on the cellular activities. The CAM has been used as an *in vivo* platform to test the tissue formation within various implants.[32,33]

The implanted collagen hydrogel was gradually incorporated into the CAM within several hours. Throughout 7 days of implantation, the collagen gel did not stimulate any host inflammatory response or vascularization as confirmed with a cell-free collagen gel (Supplementary Fig. S5). Similarly, the HDF-encapsulating collagen–PEGDE hydrogel minimally stimulated host inflammation (Fig. 7B-1). In contrast, the HDF-encapsulating collagen gel stimulated host inflammation marked by fibrous tissues around the implant (indicated by arrows) (Fig. 7A-1 and Supplementary Fig. S6B). Additionally, all cell-encapsulating hydrogel implants became more opaque and also stimulated vascularization. However, the number density of blood vessels was mediated by gel stiffness (Fig. 7A-1 & B-1). The HDF-encapsulating collagen–PEGDE hydrogel increased the density of blood vessels 1.5 times larger than the HDF-encapsulating collagen gel (Supplementary Fig. S6). We suggest that such an increase in vascular density should not result from a difference of the gel's capacity to sequester or release proangiogenic factors, because incorporation of PEGDE in the collagen gel minimally changed a diffusion coefficient of biopolymers with similar molecular weights to proangiogenic growth factors. It is likely that matrix properties mediate cellular activities, including proangiogenic factor secretion and endothelial lumen formation, although underlying mechanism should be systematically studied in future studies.

Interestingly, imaging analysis of the explants at varied length scales showed that hydrogel stiffness influenced the quality of tissues created within the gel. According to 3D images of the gel explants acquired with OCT, the collagen–PEGDE gel with *E* of 1.6 kPa displayed a more uniform matrix distribution than the pure collagen gel with *E* of 0.7 kPa, as represented by a uniform distribution of scattering

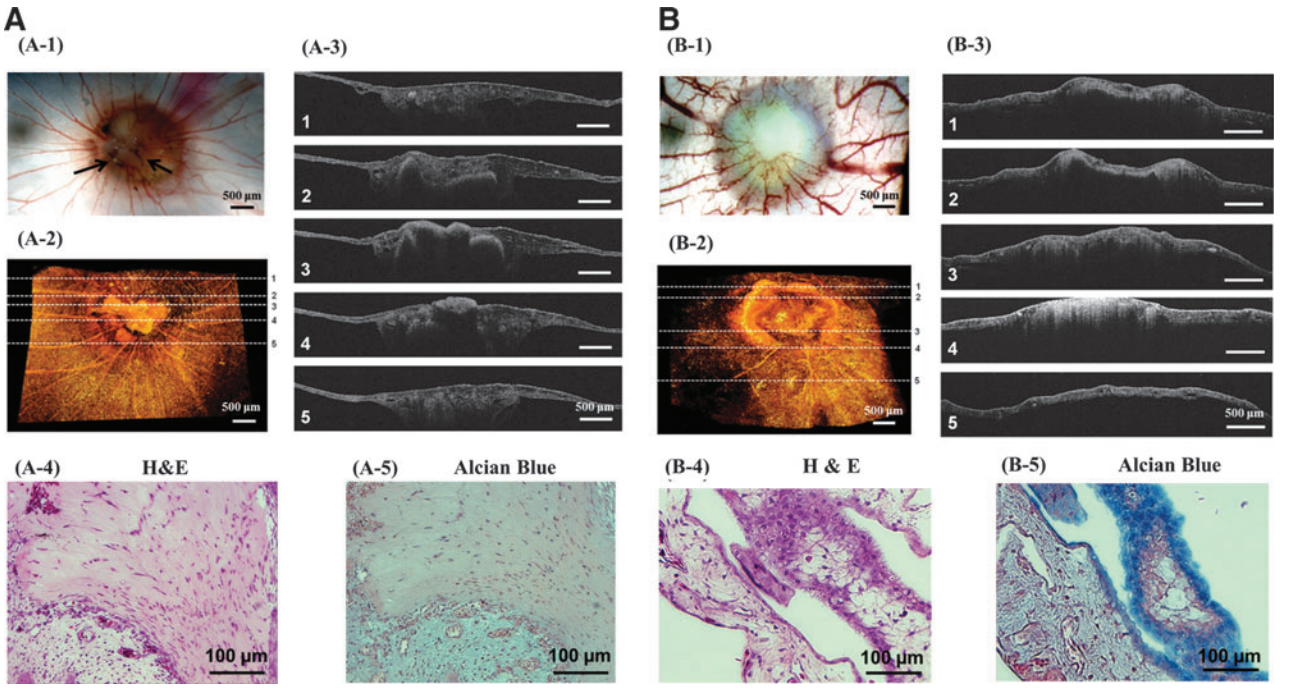

FIG. 7. *In vivo* analysis of the HDF-encapsulated hydrogels with varied *E* of 0.7 **(A)** and 1.6 kPa **(B)** following implantation on chorioallantoic membrane (CAM) over 7 days. (A-1) and (B-1): Top views of implants on CAM; (A-2) and (B-2): 3D optical coherence tomography (OCT) images of the implants on CAM; (A-3) and (B-3): Cross-sectional OCT images of implants at different positions marked in images (A-2) and (B-2). (A-4) and (B-4): Cross sections of the implants stained with hematoxylin and eosin (H&E); (A-5) and (B-5): Cross sections of the implants stained with Alcian blue.

OCT signals through the explants (Fig. 7A-2 & A-3 and 7B-2 & B-3). The heterogeneous matrix distribution in the pure collagen gel is likely due to poor resistance against cell-exerted forces and subsequent matrix shrinkage.

Additionally, cross sections of the pure collagen gel explants, stained with H&E, displayed fibrous tissue consisting of cells with stretched nuclei, similar to scar tissue (Fig. 7A-4). This result may be correlated to more active fibroblast stretching and proliferation in the softer collagen hydrogel characterized *in vitro*. In contrast, cross sections of the collagen–PEGDE gel explant exhibited cellular organization significantly different from the pure collagen gel (Fig. 7B-4).

More interestingly, the collagen–PEGDE gel explants displayed accumulation of GAG molecules, positively stained by Alcian blue, within the membrane layer (Fig. 7B-5). In contrast, the pure collagen gel explants showed few positive staining of GAG molecules (Fig. 7A-5). These results clearly indicate that dermal fibroblasts encapsulated in the stiffer collagen–PEGDE hydrogel with *E* of 1.6 kPa actively produced the GAG molecules at an implantation site, similar to *in vitro* studies.

Conclusion

This study demonstrates that mechanical stiffness of a collagen hydrogel can act as a signal to regulate morphology, growth rate, and GAG production of dermal fibroblasts loaded in the 3D gel matrix. It is proposed that the softer hydrogel with *E* of 0.7 kPa supports cell and nuclear stretching as well as proliferation in a 3D matrix. In contrast, cellular GAG production was promoted within the stiffer collagen–PEGDE hydrogels with *E* of 1.6 to 2.2 kPa, thus remodeling the gel to exhibit the enhanced water retention. Furthermore, the stiffer HDF-encapsulating collagen–PEGDE gel implanted into a living tissue created dermis-like tissue with larger GAG accumulation and vascular density than the softer gel. In the end, we envisage that the results of this study will be highly useful to better understanding the role of matrix stiffness in creating an advanced matrix for skin repair and regeneration. Furthermore, this study will serve to improve strategies to design tissue engineering scaffolds to regenerate a wide array of tissues.

Acknowledgment

This work was supported by the Amore Pacific Corporation (H.K.) and the National Science Foundation (CAREER: DMR-0847253 to H.K., CBET 10-33906 to S.B. & H.K., CBET 08-52658 ARRA to S.B., and Emerging Behaviors in Integrated Cellular Systems Grant: CBET-0939511 to H.K.) and the Research Fund of the UNIST.

Disclosure Statement

No competing financial interests exist.

References

1. Ruoslahti, E., and Pierschbacher, M.D. New perspectives in cell adhesion: RGD and integrins. Science **238,** 491, 1987.
2. Geiger, B., and Bershadsky, A. Exploring the neighborhood: adhesion-coupled cell mechanosensors. Cell **110,** 139, 2002.
3. Chiquet, M. Regulation of extracellular matrix gene expression by mechanical stress. Matrix Biol **18,** 417, 1999.
4. Rebecca, G.W. The role of matrix stiffness in regulating cell behavior. Hepatology **47,** 1394, 2008.

5. Dennis, P.M., Gordon, A.S., John, T.E., Kiran, B., Curt, M., Chung, K.H., and Anne, L.P. The stiffness of collagen fibrils influences vascular smooth muscle cell phenotype. Biophys J **92,** 1759, 2007.
6. Kong, H.J., and Mooney, D.J. Cellular microenvironments to regulate biomacromolecular therapies. Nat Rev Drug Discov **6,** 455, 2007.
7. Discher, D.E., Janmey, P., and Wang, Y.L. Tissue cells feel and respond to the stiffness of their substrate. Science **310,** 1139, 2005.
8. Donny, H.P., Vivek, B., Shen, Y.I., Jane, Y., Sudhir, K., Karen, F.T., Charles, S., Jason, A., and Sharon, G. Controlled activation of morphogenesis to generate a functional human microvasculature in a synthetic matrix. Blood **118,** 804, 2011.
9. Geiger, B., Spatz, J.P., and Bershadsky, A.D. Environmental sensing through focal adhesions. Nat Rev Mol Cell Biol **10,** 21, 2009.
10. Tibbitt, M.W., and Anseth, K.S. Hydrogels as extracellular matrix mimics for 3D cell culture. Biotechnol Bioeng **103,** 665, 2009.
11. Ruijgrok, J.M., De Wijn, J.R., and Boon, M.E. Glutaraldehyde crosslinking of collagen: effects of time, temperature, concentration and presoaking as measured by shrinkage temperature. Clin Mater **17,** 23, 1994.
12. Garcia, Y., Hemantkumar, N., Collighan, R., Griffin, M., Rodriguez-Cabello, J.C., and Pandit, A. *In vitro* characterization of a collagen scaffold enzymatically cross-linked with a tailored elastin-like polymer. Tissue Eng Part A **15,** 887, 2009.
13. David, Y.S.C., Russell, J.C., Elisabetta, A.M.V., Victoria, L.A., and Griffin, M. The cellular response to transglutaminase-cross-linked collagen. Biomaterials **26,** 6518, 2005.
14. Liang, Y., Jeong, J.H., DeVolder, R.J., Cha, C., Wang, F., Tong, Y.W., and Kong, H.J. A cell-instructive hydrogel to regulate malignancy of 3D tumor spheroids with matrix rigidity. Biomaterials **32,** 9308, 2011.
15. Tai-Lan, T., Lia, C.K., David, S., Marcel, E.N., and David, C. Dermal fibroblasts activate keratinocyte outgrowth on collagen gels. J Cell Sci **107,** 2285, 1994.
16. Scott, J.E. Structure and function in extracellular matrices depend on interactions between anionic glycosaminoglycans. Pathol Biol **49,** 284, 2001.
17. Joshua, J.L., Dan, T.S., Jeremy, J.M., Brett, Z., Michael, S.S., and Narendra, R.V. Stability and function of glycosaminoglycans in porcine bioprosthetic heart valves. Biomaterials **27,** 1507, 2006.
18. Sangmyung, R., and Federick, G. Fibroblast mechanics in 3D collagen matrices. Adv Drug Deliv Rev **59,** 1299, 2007.
19. Brian, M.G., Jacob, A.J., Meixin, W., Jason, T., and Samuel, K.S. Dynamic hydrogels: switching of 3D microenvironments using two-component naturally derived extracellular matrices. Adv Mater **22,** 686, 2010.
20. Paul, W. The quantitative measurement of Alcian Blue-glycosaminoglycan complexes. Biochem J **13,** 343, 1973.
21. Jeong, J.H., Chan, V., Cha, C., Zorlutuna, P., Dyck, C., Hsia, K.J., Bashir, R., and Kong, H.J. 'Living' microvascular stamp for patterning of functional neovessels; orchestrated control of matrix property and geometry. Adv Mater **24,** 58, 2012.
22. Boppart, S.A. Optical coherence tomography: technology and applications for neuroimaging. Psychophysiology **40,** 529, 2003.
23. Thomas, A.K., Thomas, M.W., Faouzi, K., Brian, S.G., and Timothy, H. Elastic moduli of breast and prostate tissues under compression. Untrasonic Imaging **20,** 260, 1998.
24. Patel, P.N., Smith, C.K., and Patrick, Jr., C.W. Rheological and recovery properties of poly(ethylene glycol) diacrylate hydrogels and human adipose tissue. J Biomed Mater Res A **73,** 313, 2005.
25. Zemel, A., Rehfeldt, F., Brown, A.E.X., Discher, D.E., and Safran, S.A. Optimal matrix rigidity for stress-fibre polarization in stem cells. Nat Phys **6,** 468, 2010.
26. Wang, N., Tytell, J.D., and Ingber, D.E. Mechanotransduction at a distance: mechanically coupling the extracellular matrix with the nucleus. Nat Rev Mol Cell Biol **10,** 75, 2009.
27. Huebsch, N., Arany, P.R., Mao, A.S., Shvartsman, D., Ali, O.A., Bencherif, S.A., Rivera-Feliciano, J., and Mooney, D.J. Harnessing traction-mediated manipulation of the cell/matrix interface to control stem-cell fate. Nat Mater **9,** 518, 2010.
28. Jennifer, S.P., Julia, S.C., Anchi, D.T., Rokhaya, D., Zheny, T., Aijun, W., and Song, L. The effect of matrix stiffness on the differentiation of mesenchymal stem cells in response to TGF-β. Biomaterials **32,** 3921, 2011.
29. Engler, A.J., Griffin, M.A., Sen, S., Bonnemann, C.G., Sweeney, H.L., and Discher, D.E. Myotubes differentiate optimally on substrates with tissue-like stiffness: pathological implications for soft or stiff microenvironments. J Cell Biol **166,** 877, 2004.
30. Penelope, C.G., and Paul, A.J. Cell type-specific response to growth on soft materials. J Appl Physiol **98,** 1547, 2005.
31. Chu, C., and Kong, H.J. Interplay of cell adhesion matrix stiffness and cell type for non-viral gene delivery. Acta Biomater **8,** 2612, 2012.
32. Jacques, W.M.M., Ferdinand, A.C.L.N., Gerard, A.J.D., Anton, F.P.M., Harry, A.J., and Johannes, L.H.E. The chick embryo chorioallantoic membrane as a model to investigate the angiogenic properties of human endometrium. Gynecol Obstet Invest **48,** 108, 1999.
33. Baiguera, S., Macchiarini, P., and Ribatti, D. Chorioallantoic membrane for *in vivo* investigation of tissue-engineered construct biocompatibility. J Biomed Mater Res Part B **100,** 1425, 2012.

Address correspondence to:
Hyunjoon Kong, PhD
Department of Chemical and Biomolecular Engineering
University of Illinois at Urbana–Champaign
Urbana, IL 61801-3602

E-mail: hjkong06@illinois.edu

Received: April 13, 2012
Accepted: December 12, 2012
Online Publication Date: March 4, 2013